ASSESSMENT OF SPRAY DISTRIBUTION UNIFORMITY OF A REMOTELY PILOTED AIRCRAFT SYSTEM SPRAYER

/

PAGTATASA NG PAGKAKAPANTAY-PANTAY NG PAMAMAHAGI NG WISIK GAMIT ANG REMOTELY PILOTED AIRCRAFT SYSTEM SPRAYER

Aldo C. VALDEZ[1)], Abdullah P. MERIALES[1)], Edgardo V. COLOMA[1)], Danilo B. MACATO[1)], Marvin M. CINENSE*[2)], Jonathan V. FABULA[2)], Wendy C. MATEO[2)], Sylvester A. BADUA[2)]

[1)] Department of Agricultural and Biosystems Engineering, College of Engineering, Central Luzon State University, Science City of Muñoz, Nueva Ecija, Philippines

[2)] Faculty of Department of Agricultural and Biosystems Engineering, College of Engineering, Central Luzon State University, Science City of Muñoz, Nueva Ecija, Philippines

Corresponding Author: Marvin M. Cinense; E-mail: marvin.cinense@clsu2.edu.ph

DOI: https://doi.org/10.35633/inmateh-78-29

Keywords: *Coefficient of Variation, Deposition, Droplet Size, Flight Speed, Precision Rice Production, Remotely Piloted Aircraft System, Spray Distribution Uniformity*

ABSTRACT

Efficient and uniform spray application is essential for effective pest management and sustainable rice production. This study evaluated the field spray uniformity of a Remotely Piloted Aircraft System (RPAS) sprayer operated at two flight speeds (3 and 5 m/s) and a constant flight altitude of 3 m above the rice canopy. Field experiments were conducted under actual crop conditions, with the experimental setup and spray operations documented to enhance methodological transparency and reproducibility. Water-sensitive papers were systematically arranged across the spray swath to collect droplet samples, and image analysis software was used to determine droplet size distribution ($Dv_{0.1}$, $Dv_{0.5}$, $Dv_{0.9}$), droplet density, deposition volume, and distribution uniformity. Results indicated that increasing flight speed reduced droplet size and slightly affected coverage uniformity. The median volumetric diameter ($Dv_{0.5}$) decreased from 255.56 µm at 3 m/s to 221.58 µm at 5 m/s, corresponding to medium–coarse and fine–medium spray classifications, respectively. Droplet density was higher at 3 m/s, whereas deposition volume was slightly greater at 5 m/s. The coefficient of variation (CV%) for $Dv_{0.5}$ remained within acceptable limits for agricultural spraying at both speeds, indicating satisfactory spray distribution. Overall, the RPAS sprayer demonstrated consistent field performance, with 3 m/s providing the most balanced combination of droplet size, coverage, and uniformity, supporting its potential as a viable alternative to conventional ground-based sprayers in precision rice production.

ABSTRAK

Ang episyente at pantay na aplikasyon ng spray ay mahalaga upang matiyak ang mabisang pagkontrol ng peste at ang napapanatiling produksyon ng palay. Sinuri sa pag-aaral na ito ang pagkakapantay ng distribusyon ng spray ng isang Remotely Piloted Aircraft System (RPAS) sprayer na pinatakbo sa dalawang bilis ng lipad (3 at 5 m/s) sa pare-parehong taas na 3 metro mula sa ibabaw ng tanim. Isinagawa ang mga pagsubok sa aktuwal na kondisyon ng palayan, at maingat na naidokumento ang kabuuang setup at operasyon upang matiyak ang malinaw at mapagkakatiwalaang metodolohiya. Naglagay ng mga water-sensitive paper sa iba't ibang bahagi ng lapad ng pag-spray upang mangolekta ng mga patak, at sinuri ang mga ito gamit ang image analysis software upang matukoy ang distribusyon ng laki ng patak ($Dv_{0.1}$, $Dv_{0.5}$, $Dv_{0.9}$), dami ng patak bawat yunit ng lugar, bolyum ng deposition, at antas ng pagkakapantay ng distribusyon. Ipinakita ng mga resulta na ang pagtaas ng bilis ng lipad ay nagbawas sa laki ng patak at bahagyang nakaapekto sa pagkakapantay ng coverage. Ang median volumetric diameter ($Dv_{0.5}$) ay bumaba mula 255.56 µm sa 3 m/s tungo sa 221.58 µm sa 5 m/s, na tumutugma sa medium–coarse at fine–medium na klasipikasyon ng spray. Mas mataas ang dami ng patak kada sentimetro kuwadrado sa 3 m/s, samantalang bahagyang mas mataas ang bolyum ng deposition sa 5 m/s. Nananatili sa katanggap-tanggap na antas ang coefficient of variation (CV%), na nagpapahiwatig ng maayos at pare-parehong distribusyon sa parehong bilis. Sa kabuuan, napatunayang may maaasahang performance ang RPAS sprayer sa field, at ang bilis na 3 m/s ang nagbigay ng pinakabalanseng resulta para sa precision rice production.

INTRODUCTION

Agriculture remains a major pillar of livelihood and food security in the Philippines, with rice production playing a central role in national self-sufficiency. However, conventional pesticide application methods in rice fields particularly knapsack and ground-based boom sprayers are often inefficient under flooded and waterlogged conditions. Irregular terrain, operator fatigue, inconsistent walking speed, and unstable nozzle positioning contribute to uneven droplet deposition and high coefficients of variation in spray distribution. These inefficiencies lead to chemical wastage, elevated production costs, environmental contamination, and increased risk of pest resistance (*García-Munguía et al., 2024*). While mechanized ground sprayers improve labor efficiency, their operational limitations in saturated soils restrict their performance reliability in irrigated rice systems.

Remotely Piloted Aircraft Systems (RPAS) have emerged as a promising mechanized alternative for pesticide application due to their capacity for low-altitude precision spraying, reduced operator exposure, and improved field accessibility. Prior studies have demonstrated that RPAS performance is influenced by operational parameters such as flight speed, altitude, nozzle configuration, and rotor-induced airflow (*Zheng et al., 2022; Matache et al., 2023*). However, much of the existing research has been conducted under controlled laboratory conditions, wind tunnel simulations, or in upland crops such as cotton and maize. These approaches often do not capture the aerodynamic complexity of flooded rice fields, where high humidity, canopy structure, thermal gradients, and rotor downwash interactions significantly affect droplet transport and deposition behavior.

A key limitation in current literature is the insufficient field-based quantification of spray distribution uniformity in tropical rice environments, particularly using standardized droplet spectrum analysis and transverse swath evaluation. Many studies emphasize deposition quantity or drift potential but do not rigorously assess uniformity indices such as coefficient of variation (CV%) across the effective swath width under actual operational conditions. Consequently, optimized flight configurations for rice systems remain inadequately defined, limiting the development of evidence-based operational guidelines.

Flight speed, in particular, is a critical but under-characterized parameter in field applications. Variations in forward speed alter rotor-induced airflow patterns, droplet breakup dynamics, and horizontal dispersion, directly affecting droplet size distribution, density, and spatial uniformity (*Zhou et al., 2021; He et al., 2021; Gao et al., 2024*). Without systematic field validation, recommended speed settings may not ensure acceptable spray uniformity thresholds required for effective pest management and environmental safety.

To address these gaps, the present study implemented a field-based experimental design incorporating transverse sampling across the spray swath using water-sensitive papers and image-based droplet spectrum analysis. By evaluating droplet size parameters ($Dv_{0.1}$, $Dv_{0.5}$, $Dv_{0.9}$), droplet density, volumetric deposition, and distribution uniformity expressed as coefficient of variation, the study provides a mechanistic assessment of how flight speed influences spray behavior under actual rice field conditions. Unlike simulation-based assessments, this approach captures real aerodynamic interactions between rotor downwash, ambient microclimate, and crop canopy.

Therefore, this study aimed to evaluate the spray distribution uniformity of an RPAS sprayer operated at different flight speeds in a tropical rice production environment. The results contribute to the development of performance-based operational benchmarks and optimized flight parameters that enhance application efficiency, uniformity, and environmental sustainability in precision rice production systems.

MATERIALS AND METHODS

Experimental Site and Conditions

The spraying trials were conducted at the Philippine-Sino Center for Agricultural Technology experimental field, in collaboration with the College of Engineering, Central Luzon State University (CLSU), Science City of Muñoz, Nueva Ecija, Philippines. The site represents a typical lowland rice ecosystem characterized by flat terrain and favorable climatic conditions, ideal for evaluating aerial spraying performance.

All experiments were performed under stable meteorological conditions to ensure consistent spray distribution and minimize environmental variability. During the trials, the ambient temperature ranged from 29.3°C to 34.5°C, with an average relative humidity of 60%, typical of tropical rice-growing regions (Table 1). The mean wind velocity ranged from 2.8 to 5.2 km/h, which is well below the recommended operational threshold of 16 km/h for RPAS-based spraying (*Qin et al., 2016; Wang et al., 2018*). These stable conditions minimized droplet drift, maintained spray plume integrity, and ensured uniform deposition across the swath.

Table 1

Weather data during the RPAS spray test

Parameters	Time, AM			
	7:00	8:00	9:00	10:00
Wind speed, km/h	2.8	3.2	3.9	5.2
Temperature, °C	29.3	32.1	34.3	34.5
Relative humidity, %	60	60	60	60
Rainfall, mm	0.0	0.0	0.0	0.0
Barometric pressure, hPa	10 017	10 017	10 017	10 017
Wind direction	Southwest	Southwest	Southwest	Southwest

Meteorological parameters were recorded hourly. Wind speed and temperature were measured using a handheld digital anemometer, while humidity, rainfall, wind direction, and barometric pressure were obtained from the PAG-ASA Weather Station at CLSU. All spraying operations were conducted between 7:00 a.m. and 10:00 a.m., following the ASABE S386.2 standard for aerial application testing.

RPAS Sprayer Description

The aerial spraying operation of the RPAS sprayer was carried out using RPAS agricultural drone equipped with and integrated liquid spraying module. The RPAS sprayer was powered by a multi-rotor configurations with six (6) rotors that were designed for agricultural use, providing stable hovering, and precise flight control. The drone is equipped with a high-precision positioning system, such as GPS, which allows it to navigate and fly autonomously over the designated agricultural area. It uses an electric pump to generate pressure and deliver the liquid to the spraying nozzles. These nozzles release the liquid in a controlled manner, ensuring even coverage of the crops.

The aerial spraying operation was conducted using a DJI Agras T30 agricultural RPAS (Model 3WWDZ-30A) equipped with an integrated liquid spraying system. The platform features a six-rotor multi-rotor configuration specifically designed for stable hovering and precise low-altitude agricultural applications. The aircraft is powered by high-torque electric motors (maximum 3600 W per rotor) and utilizes a high-precision GNSS-based positioning system for autonomous navigation and accurate flight path control.

The spraying system consists of a 30-L spray tank, dual plunger pumps, and a multi-nozzle boom assembly. The electric pump system generates and regulates spray pressure, delivering pressurized liquid uniformly to sixteen (16) XR 11001VS flat-fan nozzles (TeeJet® Technologies) mounted beneath the rotor arms. These nozzles are widely recommended for pesticide applications due to their ability to produce fine-to-medium droplet spectra, enabling effective coverage while maintaining drift control (Fritz et al., 2014; Nuyttens et al., 2007; Wang et al., 2020). The selected nozzle configuration ensures adequate overlap between adjacent spray patterns and uniform deposition across the effective spray width (4–9 m).

Spray pressure was regulated using the on-board pump control system and maintained consistently across all replications to minimize variability in droplet formation. Prior to field testing, nozzle flow rate uniformity was verified using a calibrated graduated cylinder and stopwatch method to confirm consistent discharge rates among all nozzles. Any nozzle with deviation beyond ±5% of the mean output was replaced to ensure system uniformity.

Fig. 1 - Machine inspection of RPAS Agricultural Drone (DJI Agras T30)

The RPAS flight path, altitude (3 m above canopy), and operating speeds (3 m/s and 5 m/s) were pre-programmed using the on-board autonomous navigation system to maintain constant operational parameters and minimize pilot-induced variability across trials.

Photographic documentation of the RPAS platform, nozzle configuration, and mounting arrangement during field operation is provided in Figure 1 to allow visual verification of the spraying system configuration and experimental setup.

The detailed technical specifications of the RPAS sprayer are presented in Table 2.

Table 2

Specification of RPAS Sprayer (Agras T30) used

Item	Specification
Model	3WWDZ-30A
Spray Tank Volume	30 L
Operating Payload	30 kg
Spray Width	4 to 9 m
No. of Pumps	2 Plunger Pumps
No. of Nozzles	12 Nozzles
Maximum Operating Speed	7 m/s
Maximum Flying Speed	10 m/s
Maximum Wind Resistance	8 m/s
Motor Max Power	3600 W/rotor
Max Working Current	60 A
Total Weight	26.4 kg (excluding battery)

Experimental Design and Field Layout

The experiment followed a completely randomized design (CRD) with two flight speeds as treatments (3 m/s and 5 m/s). Each treatment was replicated three times, for a total of six test flights. Data were summarized using descriptive statistics to assess variation across sampling points, and an independent t-test was used to determine significant differences between flight speeds.

The experiment was conducted according to the American Society of Agricultural and Biological Engineer (ASABE) Standard S386.2 (R2018) for measuring spray pattern uniformity in aerial applications. The RPAS sprayer operated at a height of 3 meter, and each trial consisted of a single flight pass along three sampling lines (S1, S2, and S3) in the same direction (Fig. 1).

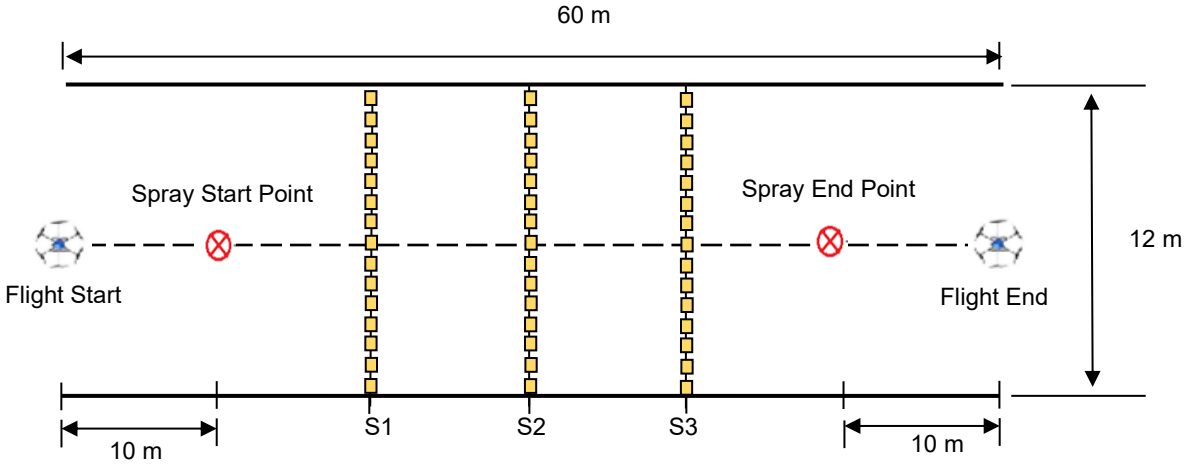

Fig. 2 - Experimental field layout

The experimental field measured 60 m × 12 m. Markers were placed at both ends to guide the flight path, and the center line was marked with flaglets to ensure alignment. Along the 60-meter path, ribbon frames were set at 10-meter intervals and secured to the ground to hold water-sensitive papers (WSPs) flat during spraying.

A scaled field layout diagram (Figure 2) and corresponding field photographs are provided to clearly illustrate the spatial arrangement of sampling lines (S1–S3), the 60 m × 12 m test plot dimensions, marker placements, and WSP mounting frames. These visual references ensure accurate replication of sampling geometry, collector spacing (0.8 m), and alignment relative to the RPAS flight trajectory.

Droplet Sampling Procedure

Water-sensitive papers (WSPs) (Syngenta®, 26 mm × 76 mm, yellow, rigid) were used to collect droplet deposition data. The WSPs were mounted horizontally at the flat ground level aligned perpendicular to the RPAS flight direction.

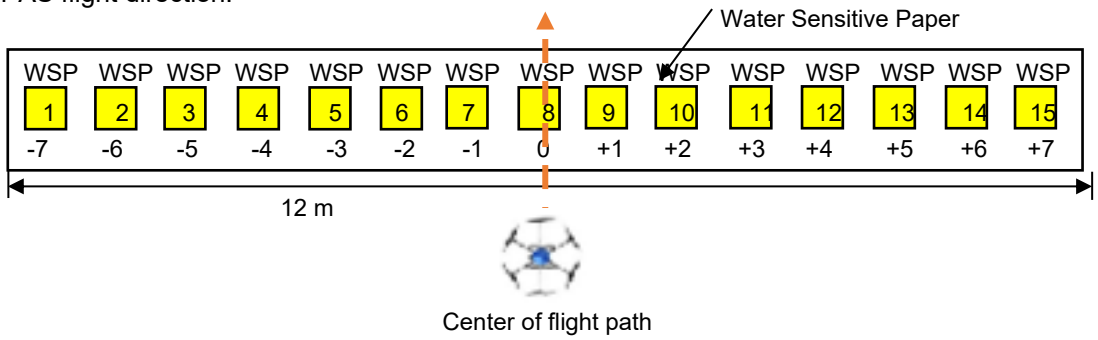

Fig. 3 - Layout of spray deposit collector (WSP).

Each sampling line consisted of 15 sampling points, spaced 0.8 m apart, following the ASABE S386.2 standard, which requires target spacing not to exceed 1 m. Sampling points were numbered from –7 to +7, where point 0 corresponded to the center of the flight path and points –7 and +7 represented the outer edges of the spray swath (Figure 3).

After spraying, the WSPs were carefully collected, air-dried, and stored in sealed plastic containers to prevent moisture contamination. All samples were handled using non-latex gloves to avoid contact residue. The dried WSPs were then analyzed for droplet density, size, and coverage using DepositScan image analysis software.

Droplet Analysis and Parameters

The collected WSPs were scanned using a flatbed scanner at 600 dpi resolution, and the images were analyzed using the DepositScan program developed by the United States Department of Agriculture – Unmanned Aircraft Systems (USDA-UAS). The following parameters were derived:

1. Volume Median Diameter (μm) - All detected droplets were sorted from smallest to largest Dv0.1, Dv0.5, and Dv0.9 will represent the volume of small, medium, and large sized droplets respectively.
2. Droplet Density (number of droplets/cm^2). This represented the number of droplets per unit area.
3. Droplet Deposition (μL/cm^2) – total spray liquid deposited per unit surface area.
4. Spray coverage (%) – proportion of surface area covered by spray droplets.

All results represent the mean of three replications per treatment.

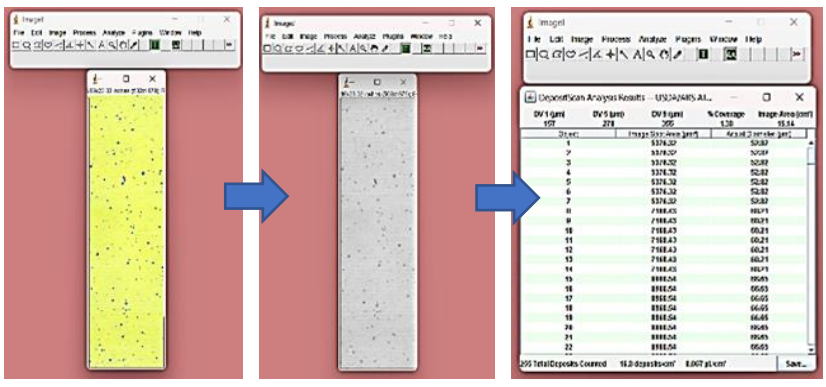

(a) (b) (c)

Fig. 3 - Flowchart of droplet deposition analysis using DepositScan software

The DepositScan software was utilized to analyze water-sensitive paper (WSP) samples for droplet characterization and quantification. This software automatically detects and measures droplet deposits from scanned WSP images, enabling accurate estimation of droplet size, density, coverage, and deposition rate. The analysis process involved importing the WSP image into DepositScan, converting the color image to an 8-bit grayscale format, defining the sample area, and selecting the green AA tool for droplet detection and measurement. The program then computed droplet deposition parameters based on pixel contrast and surface coverage. The flowchart of the analysis procedure is presented in Figure 3, which illustrates the sequential steps: (a) importing the WSP image, (b) image conversion and area marking, and (c) droplet analysis using the green AA tool.

Droplet size distribution was determined using the volumetric diameters $Dv_{0.1}$, $Dv_{0.5}$, and $Dv_{0.9}$, representing the droplet diameters at which 10%, 50%, and 90% of the total spray volume is contained, respectively. Among these, $Dv_{0.5}$ the Volume Median Diameter (VMD) was used as the principal indicator of spray quality. It defines the midpoint of the droplet spectrum, where half of the total spray volume comprises droplets smaller than $Dv_{0.5}$ and half larger. This parameter is widely applied in spray technology for classifying spray categories (ASABE S572.1) and evaluating the trade-off between drift potential and canopy coverage efficiency.

Table 3

Droplet size classification based on ASABE Standard S572.1 (2020)

Droplet Size Classification	Range, $Dv_{0.5}$ (μm)	Classification Description
Very Fine (VF)	< 150	High drift potential; fine mist-like spray
Fine (F)	150 – 235	Good coverage; moderate drift risk
Medium (M)	236 – 340	Balanced coverage and drift control
Coarse (C)	341 – 403	Reduced drift; suitable for canopy spraying
Very Coarse (VC)	404 – 502	Limited drift; lower coverage uniformity
Extremely Coarse (XC)	503 – 665	Minimal drift; large droplet deposition
Ultra Coarse (UC)	> 665	Minimal drift; large droplets, low coverage

The $Dv_{0.1}$ and $Dv_{0.9}$ parameters were also analyzed to characterize fine, drift-prone droplets and coarse, canopy-penetrating droplets, respectively, providing a comprehensive assessment of droplet size distribution and uniformity (Table 3.)

Droplet deposition, expressed in microliters per square centimeter (μL/cm²), was used to quantify the spray liquid retained on the target surface. Smaller droplets (<150 μm) generally enhance surface coverage but are more prone to drift, while larger droplets (>200 μm) reduce drift but may produce uneven coverage. Therefore, achieving an optimal droplet size is essential to balance coverage efficiency, drift control, and application uniformity (*Garcia-Munguia et al., 2024*).

The results were evaluated against standard aerial spraying benchmarks, which define effective application as having a droplet density of 20–40 droplets/cm², deposition of 0.05–0.20 μL/cm², and spray coverage exceeding 1% (*Wang et al., 2018; Zhang et al., 2021*).

Distribution Uniformity (CV %)

The distribution uniformity of spray droplet sizes was assessed using the coefficient of variation (CV) as a key statistical indicator to quantify the degree of variability in droplet size and deposition across sampling points within the spray swath. The CV provides a dimensionless measure of relative dispersion, calculated as the ratio of the standard deviation to the mean, thereby allowing comparisons between datasets with different magnitudes or units. It serves as an effective performance metric for evaluating the consistency of spray application across the target area.

A lower CV value denotes a more uniform and stable droplet distribution, while a higher CV indicates greater variability and uneven deposition. According to established agricultural spray application standards, a CV below 15% reflects high uniformity, while values between 15% and 30% indicate moderate uniformity (*ASAE EP458, 1989; ASABE S572.1, 2020*). In general, a CV not exceeding 20% is considered acceptable for field spraying operations, as this range ensures adequate coverage and minimizes the risk of over- or under-application of agrochemicals (*ASAE Standards, 2003; Nuyttens et al., 2007*). These thresholds provide a quantitative benchmark for assessing spray quality in aerial and ground-based application systems.

In this study, the CV values were calculated for each of the droplet size parameters $Dv_{0.1}$, $Dv_{0.5}$, and $Dv_{0.9}$, representing the 10th, 50th, and 90th percentiles of the cumulative droplet size distribution, respectively. This approach enabled a comprehensive evaluation of spray uniformity across the fine, median, and coarse droplet classes. The $Dv_{0.1}$ represents the fraction of smaller droplets most prone to drift, $Dv_{0.5}$ corresponds to the median droplet size that best characterizes the spray pattern, and $Dv_{0.9}$ reflects the larger droplets that contribute to penetration and deposition efficiency.

By computing the CV for each percentile class at both 3 m/s and 5 m/s flight speeds, the study quantified the extent of droplet size variation attributable to flight dynamics and aerodynamic turbulence. This comparative analysis allowed for a detailed understanding of how flight speed influences atomization behavior, droplet breakup uniformity, and overall spray consistency under field conditions.

This analytical framework ensured precise characterization of spray distribution uniformity and provided a robust basis for evaluating the performance efficiency of the RPAS sprayer under varying operational flight speeds. The results derived from these indices were subsequently used to interpret the aerodynamic stability and spray consistency of the RPAS system across different droplet size spectra. The coefficient of variation for each droplet size class was calculated using Equations (1), (2), and (3).

$$\bar{X} = \left(\frac{\sum Xi}{n}\right) \quad (1)$$

$$Standard\ deviation = \sqrt{\frac{\sum(x_i - \bar{X})^2}{(n-1)}} \quad (2)$$

$$CV = \frac{Standard\ deviation}{\bar{X}}\ (100\%) \quad (3)$$

where: $\bar{X}$ is the arithmetic mean droplet size across sapling points, X_i is the quantified deposit for one sampling point and n denotes the number of sampling point.

RESULTS

Droplet Size Characteristics

Tables 4 and 5 present the mean droplet deposition at each sampling point under different flight speeds, as determined from water-sensitive paper (WSP) analysis using the DepositScan program. The droplet size distribution was characterized by $Dv_{0.1}$, $Dv_{0.5}$, and $Dv_{0.9}$, which represent the 10th, 50th, and 90th percentiles of the droplet diameter, respectively. Additionally, droplet density (droplets/cm²) and deposition (µL/cm²) were quantified to assess the spray pattern across the swath.

Scanned water-sensitive papers (WSPs) taken after each spray pass are presented in Figures 4 and 5. These images visually confirm the numerical trends, showing denser and more uniformly distributed droplet stains at 3 m/s compared with the more concentrated central deposition observed at 5 m/s.

Table 4

Mean droplet deposition in the spraying test at 3 m/s flight speed

Sample Point	Spray Droplet Size (µm)			Droplet Density (number of droplets/cm²)	Deposition (µL/cm²)
	Dv0.1	Dv0.5	Dv0.9		
-7	105.33	213.00	333.00	5.60	0.005
-6	127.00	236.00	340.33	10.03	0.010
-5	132.00	254.33	383.67	15.20	0.022
-4	130.33	221.33	320.00	18.50	0.027
-3	139.67	252.67	366.33	46.83	0.080
-2	138.67	255.67	358.67	54.23	0.084
-1	140.00	240.33	361.00	50.87	0.082
0	159.00	279.67	416.00	38.37	0.086
1	153.33	292.67	451.00	42.00	0.155
2	155.00	296.00	437.67	47.83	0.152
3	160.67	283.67	460.33	40.63	0.094
4	134.67	243.67	426.33	21.60	0.052
5	145.33	265.67	410.00	22.87	0.041
6	132.33	245.67	405.00	17.23	0.038
7	168.33	253.00	350.33	6.53	0.010

Values represent the mean of three replications.

Table 5

Mean droplet deposition in the spraying test at 5 m/s flight speed

Sample Point	Spray Droplet Size (μm)			Droplet Density (number of droplets/cm²)	Deposition (μL/cm²)
	Dv 0.1	Dv 0.5	Dv 0.9		
-7	83.67	173.33	237.33	9.30	0.014
-6	89.00	164.00	284.00	9.83	0.021
-5	104.33	210.67	321.33	9.97	0.023
-4	111.33	203.67	315.33	12.60	0.028
-3	137.33	224.33	381.67	15.97	0.038
-2	120.00	209.67	328.33	16.47	0.043
-1	118.67	220.00	367.67	21.63	0.056
0	171.00	274.67	474.33	48.07	0.212
1	158.33	280.33	450.67	39.03	0.168
2	158.67	279.33	431.67	42.83	0.165
3	137.67	233.33	371.00	41.43	0.203
4	135.33	225.67	372.33	31.67	0.100
5	118.33	209.67	322.67	32.63	0.100
6	125.00	212.00	358.33	19.00	0.046
7	91.00	203.00	286.67	2.40	0.009

Values represent the mean of three replications.

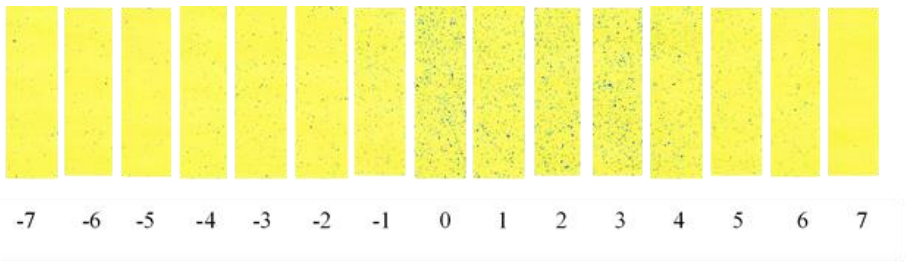

Fig. 4 -Scanned WSP at 3 m/s flight speed

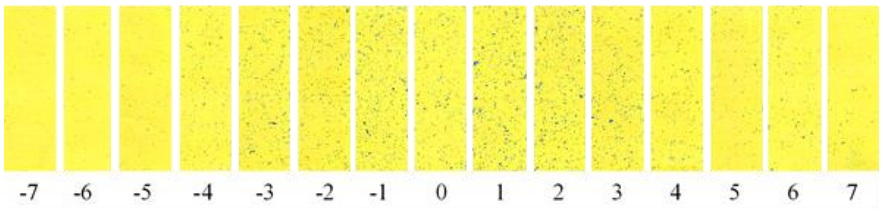

Fig. 5 - Scanned WSP at 5 m/s flight speed

At 3 m/s, droplet deposition exhibited a relatively symmetrical distribution about the centerline (sample point 0), with gradual reduction toward the swath edges (−7 and +7). In contrast, at 5 m/s, deposition intensity was strongly concentrated near the centerline, with a steeper decline toward the outer sampling points. This visual pattern, documented in the photographs, supports the numerical evidence of reduced lateral spread at higher flight speed.

Table 6

Mean droplet distribution indices under two flight speeds

Flight Speed (m/s)	$Dv_{0.1}$(μm)	$Dv_{0.5}$ (μm)	$Dv_{0.9}$ (μm)	Spray Classification
3	141.44	255.56	387.98	Medium to Coarse
5	123.98	221,58	353.56	Fine to Medium

Values represent the mean of three replications.

These results indicate that increasing flight speed reduced droplet size, particularly in the finer and median portions of the spray spectrum. The 3 m/s flight speed produced droplets classified as medium–coarse, whereas 5 m/s generated fine–medium droplets. The trend demonstrates that lower flight speeds favor the formation of larger droplets, resulting in greater mass per droplet and potentially reduced drift, while higher speeds promote finer atomization due to stronger aerodynamic forces and increased airflow turbulence beneath the rotor. Consequently, droplet breakup becomes more pronounced at 5 m/s, enhancing spray coverage but possibly increasing drift risk under field conditions.

Droplet Distribution Evaluation Indices

Table 7 presents the mean droplet density, deposition, and surface coverage obtained under two flight speeds. At a flight speed of 3 m/s, the mean droplet density was 29.21 droplets/cm², while at 5 m/s it was 23.52 droplets/cm². The corresponding mean droplet deposition values were 0.063 µL/cm² and 0.082 µL/cm², whereas surface coverage averaged 1.66% and 1.40%, respectively.

Results showed no significant differences in droplet density and deposition between the two flight speeds, indicating that the overall spray volume per unit area remained consistent regardless of the operational speed. However, notable differences in droplet distribution patterns were observed. The lower flight speed (3 m/s) produced a higher droplet density and greater surface coverage, signifying a more uniform distribution and improved wetting efficiency across the spray swath. This condition suggests that the slower flight speed allowed droplets more time to settle uniformly on the target surface, minimizing drift and enhancing coverage uniformity.

Table 7

Mean droplet density, deposition, and coverage under two flight speeds.

Flight Speed (m/s)	Droplet Density (no. of Droplets/cm²)	Deposition (µL/cm²)	Spray Coverage (%)
3	29.22	0.063	1.60
5	23.52	0.082	1.44

Values represent the mean of three replications.

Conversely, the higher flight speed (5 m/s) resulted in a slightly greater deposition volume but lower droplet density and coverage. This implies that while the total spray liquid deposited per unit area was somewhat higher, the droplets were more concentrated near the flight path centerline, indicating reduced lateral spread and a narrower effective swath width. The stronger downdraft and increased airflow velocity at 5 m/s likely promoted droplet coalescence and localized accumulation directly beneath the flight line.

All measured parameters on droplet density, deposition, and surface coverage met acceptable standards for effective aerial spraying, confirming the satisfactory spray performance of the RPAS sprayer at both flight speeds. The results emphasize that 3 m/s flight speed provides more uniform spray distribution, while 5 m/s offers slightly higher deposition intensity, suggesting that operational flight speed can be optimized depending on the desired balance between coverage uniformity and deposition concentration in aerial spraying applications.

Distribution Uniformity

Table 8 presents the coefficient of variation (CV %) for the droplet size parameters $Dv_{0.1}$, $Dv_{0.5}$, and $Dv_{0.9}$ under the two flight speeds. The coefficient of variation (CV%) values (Table 8) clearly demonstrate the influence of flight speed on droplet uniformity. At 3 m/s, all CV values were below 12%, indicating high uniformity. At 5 m/s, CV values increased (15–21%), reflecting greater droplet spectrum variability.

The increase in variability at higher speed is consistent with aerodynamic theory. As forward velocity increases, rotor-induced downwash interacts more intensely with horizontal airflow, producing turbulence gradients beneath the aircraft. This results in irregular droplet breakup and non-uniform spatial dispersion. The WSP photographs visually corroborate this effect, showing slightly more heterogeneous droplet imprint distribution at 5 m/s.

Despite increased variability at higher speed, all CV values remained within acceptable agricultural spraying limits (<30%), confirming that the RPAS sprayer maintained operational stability under both treatments.

Table 8

Distribution uniformity indices of droplet sizes at two different flight speed.

Parameter	Spray Droplet Size (μm)		
	$Dv_{0.1}$	$Dv_{0.5}$	$Dv_{0.9}$
DU (CV%) at 3 m/s, %	11.35	9.55	11.55
DU (CV%) at 5 m/s, %	21.17	15.53	18.31

The results showed that droplet size uniformity decreased as flight speed increased, likely due to greater aerodynamic turbulence and airflow instability beneath the rotor downwash. Higher airspeed may have caused uneven atomization at the nozzles, producing a wider droplet size range. In contrast, the lower flight speed of 3 m/s produced a more stable spray plume and finer atomization control, resulting in a narrower droplet spectrum and improved uniformity across the swath.

The RPAS sprayer maintained stable droplet size distribution across both flight speeds, with superior uniformity and consistency observed at 3 m/s. This indicated that the lower flight speed provided more favorable spraying conditions, promoting uniform droplet formation and consistent deposition.

Variability between Replications

Across the three replications per treatment, variability remained within acceptable limits. Standard deviations were modest relative to mean values, particularly at 3 m/s. Slightly higher variation at 5 m/s was observed, which is reflected in the increased CV values (Table 8). This indicates that higher flight speed amplified sensitivity to minor fluctuations in rotor stability and ambient airflow conditions.

Influence of Environmental Conditions

Meteorological parameters remained within controlled limits throughout testing. Wind speed (2.8–5.2 km/h) was below the recommended maximum threshold and did not cause observable drift beyond the sampling boundary. However, slight directional variability in wind may have contributed to minor asymmetry between the left and right swath edges in some replications, particularly at 5 m/s, where droplet transport is more sensitive to horizontal airflow components.

Relative humidity (approximately 60%) likely reduced rapid droplet evaporation, maintaining droplet integrity prior to impact. The combination of moderate humidity and low wind conditions helped isolate the influence of flight speed as the primary experimental variable.

CONCLUSIONS

The RPAS sprayer achieved effective aerial application under low-altitude field conditions. Flight speed significantly affected droplet size and distribution: 3 m/s produced medium–coarse droplets with high uniformity, while 5 m/s generated finer droplets with slightly greater variability. Droplet density, deposition, and surface coverage remained within acceptable ranges for both speeds. The results demonstrate that lower flight speeds optimize spray uniformity and coverage, whereas higher speeds increase atomization but may reduce lateral spread. Overall, the RPAS sprayer showed reliable and consistent performance, supporting its potential as an alternative to conventional ground sprayers for precision rice production.

ACKNOWLEDGEMENT

The authors would like to express their gratitude to the Engineering Research and Development for Technology (ERDT) at the Department of Science and Technology (DOST) for providing financial support, to the Department of Agricultural and Biosystem Engineering, College of Engineering, Central Luzon State University and to the Central Luzon State University - Center for hybrid Rice Research, Innovation, and Mechanization (CLSU-CHRRIM) staff for the completion of this study.

REFERENCES

[1] ASAE EP458. (1989). *Spray nozzle classification by droplet spectra*. American Society of Agricultural Engineers, St. Joseph, MI, USA.

[2] ASAE Standards. (2003). *ASAE S327.2: Terminology and definitions for agricultural chemical application*. American Society of Agricultural Engineers, St. Joseph, Michigan, USA.

[3] ASABE. (2020). S386.2 (R2018): *Test procedure for determining the uniformity of water distribution from aerial application equipment*. St. Joseph, MI: ASABE.

[4] ASABE. (2020). *ASABE Standards S572.1: Spray Nozzle Classification by Droplet Spectra*. American Society of Agricultural and Biological Engineers.

[5] Byers, C., Virk, S., Rains, G., & Li, S. (2024). Spray deposition and uniformity assessment of unmanned aerial application systems (UAAS) at varying operational parameters. *Frontiers in Agronomy*, 6, 1418623. https://doi.org/10.3389/fagro.2024.1418623

[6] Fritz, B. K., Hoffmann, W. C., & Bagley, W. E. (2014). Effects of spray mixture on droplet size under aerial application conditions. *Transactions of the ASABE*, 57(5), 1345–1351.

[7] Gao, Y., He, X., Yan, Q., Zeng, A., & Wang, C. (2024). Droplet deposition characteristics of an unmanned aerial spraying system at different flight parameters. *Biosystems Engineering*, 238, 25–36.

[8] García-Munguía, A., Guerra-Ávila, P. L., Islas-Ojeda, E., Flores-Sánchez, J. L., Vázquez-Martínez, O., García-Munguía, A.M., & García-Munguía, O. (2024). A review of drone technology and operation processes in agricultural crop spraying. *Drones*, 8(11), 674. https://doi.org/10.3390/drones8110674

[9] He, X., Bonds, J., Herbst, A., & Langenakens, J. (2021). Recent development of unmanned aerial vehicle systems for pesticide application in agriculture. *Outlooks on Pest Management*, 32(1), 13–19.

[10] Li, S., Byers, C., & Rains, G. (2023). DepositScan software for quantifying droplet size, density, and deposition in UAV spraying tests. *Transactions of the ASABE*, 66(4), 567–576.

[11] Matache, M. G., Găgeanu, I., Gheorghe, G. V., Persu, C., Chiriițescu, M., & Nițu, M. (2023). Development of a tricopter-hexarotor agricultural UAV destined for realization of precision spraying works. *INMATEH Agricultural Engineering*, 70(2), 11–20. https://doi.org/10.35633/inmateh-70-01

[12] Nuyttens, D., Baetens, K., De Schampheleire, M., Sonck, B., & Meirvenne, M. V. (2007). Effect of nozzle type, size, and pressure on spray droplet characteristics. *Biosystems Engineering*, 97(3), 333–345.

[13] Qin, W.C., Xue, X.Y., Zhang, S.C., Gu, W. & Wang, B. (2016). Droplet deposition and drift of aerial spraying by unmanned aerial vehicle. *International Journal of Agricultural and Biological Engineering*, 9(4), 58–66.

[14] Wang, J., Lan, Y., & Zhang, H. (2018). Effect of flight parameters on spray drift and deposition in UAV-based applications. *Transactions of the ASABE*, 61(6), 1823–1830.

[15] Wang, L., Tang, Q., Li, J., & Zhang, R. (2020). Optimization of nozzle configurations for UAV pesticide applications. *Computers and Electronics in Agriculture*, 178, 105760.

[16] Wu, T., Li, Y., & Zhang, J. (2020). Water-sensitive paper and image analysis for aerial spray uniformity evaluation. *Precision Agriculture*, 21, 1152–1166. https://doi.org/10.1007/s11119-020-09749-3

[17] Zhang, D., Lan, Y., Chen, P., & Wang, J. (2021). Evaluation of spray deposition and drift from agricultural UAVs under variable flight parameters. *International Journal of Agricultural and Biological Engineering*, 14(2), 15–22. https://doi.org/10.25165/j.ijabe.20211402.6152

[18] Zhang, S., Wang, C., & He, X. (2022). Field performance and drift control of UAV-based spraying systems. *Agricultural Engineering International: CIGR Journal*, 24(1), 65–74.

[19] Zheng, J., Li, Y., Zhang, L., & Xue, X. (2022). Analysis of roll stability of the sprayer based on the equivalent mechanical model of liquid sloshing. *INMATEH Agricultural Engineering*, 67(2), 106–116. https://doi.org/10.35633/inmateh-67-10

[20] Zheng, J., Li, Y., & Zhang, L. (2021). Visual documentation of UAV spray distribution using water-sensitive papers. *Computers and Electronics in Agriculture*, 185, 106120.

[21] Zhou, Z., He, X., & Liu, J. (2021). Influence of operational parameters on spray deposition of unmanned aerial spraying systems. *Computers and Electronics in Agriculture*, 187, 106269.